Direct measurement of the mass difference between top and antitop quarks

V.M. Abazov, B. Abbott, M. Abolins, B.S. Acharya, M. Adams, T. Adams, E. Aguilo, M. Ahsan, G.D. Alexeev, G. Alkhazov, et al.

Direct measurement of the mass difference between top and antitop quarks

V.M. Abazov[37], B. Abbott[75], M. Abolins[65], B.S. Acharya[30], M. Adams[51], T. Adams[49], E. Aguilo[6], M. Ahsan[59], G.D. Alexeev[37], G. Alkhazov[41], A. Alton[64,a], G. Alverson[63], G.A. Alves[2], L.S. Ancu[36], T. Andeen[53], M.S. Anzelc[53], M. Aoki[50], Y. Arnoud[14], M. Arov[60], M. Arthaud[18], A. Askew[49,b], B. Åsman[42], O. Atramentov[49,b], C. Avila[8], J. BackusMayes[82], F. Badaud[13], L. Bagby[50], B. Baldin[50], D.V. Bandurin[59], S. Banerjee[30], E. Barberis[63], A.-F. Barfuss[15], P. Bargassa[80], P. Baringer[58], J. Barreto[2], J.F. Bartlett[50], U. Bassler[18], D. Bauer[44], S. Beale[6], A. Bean[58], M. Begalli[3], M. Begel[73], C. Belanger-Champagne[42], L. Bellantoni[50], A. Bellavance[50], J.A. Benitez[65], S.B. Beri[28], G. Bernardi[17], R. Bernhard[23], I. Bertram[43], M. Besançon[18], R. Beuselinck[44], V.A. Bezzubov[40], P.C. Bhat[50], V. Bhatnagar[28], G. Blazey[52], S. Blessing[49], K. Bloom[67], A. Boehnlein[50], D. Boline[62], T.A. Bolton[59], E.E. Boos[39], G. Borissov[43], T. Bose[62], A. Brandt[78], R. Brock[65], G. Brooijmans[70], A. Bross[50], D. Brown[19], X.B. Bu[7], D. Buchholz[53], M. Buehler[81], V. Buescher[22], V. Bunichev[39], S. Burdin[43,c], T.H. Burnett[82], C.P. Buszello[44], P. Calfayan[26], B. Calpas[15], S. Calvet[16], J. Cammin[71], M.A. Carrasco-Lizarraga[34], E. Carrera[49], W. Carvalho[3], B.C.K. Casey[50], H. Castilla-Valdez[34], S. Chakrabarti[72], D. Chakraborty[52], K.M. Chan[55], A. Chandra[48], E. Cheu[46], D.K. Cho[62], S. Choi[33], B. Choudhary[29], T. Christoudias[44], S. Cihangir[50], D. Claes[67], J. Clutter[58], M. Cooke[50], W.E. Cooper[50], M. Corcoran[80], F. Couderc[18], M.-C. Cousinou[15], S. Crépé-Renaudin[14], D. Cutts[77], M. Ćwiok[31], A. Das[46], G. Davies[44], K. De[78], S.J. de Jong[36], E. De La Cruz-Burelo[34], K. DeVaughan[67], F. Déliot[18], M. Demarteau[50], R. Demina[71], D. Denisov[50], S.P. Denisov[40], S. Desai[50], H.T. Diehl[50], M. Diesburg[50], A. Dominguez[67], T. Dorland[82], A. Dubey[29], L.V. Dudko[39], L. Duflot[16], D. Duggan[49], A. Duperrin[15], S. Dutt[28], A. Dyshkant[52], M. Eads[67], D. Edmunds[65], J. Ellison[48], V.D. Elvira[50], Y. Enari[77], S. Eno[61], M. Escalier[15], H. Evans[54], A. Evdokimov[73], V.N. Evdokimov[40], G. Facini[63], A.V. Ferapontov[59], T. Ferbel[61,71], F. Fiedler[25], F. Filthaut[36], W. Fisher[50], H.E. Fisk[50], M. Fortner[52], H. Fox[43], S. Fu[50], S. Fuess[50], T. Gadfort[70], C.F. Galea[36], C. Garcia[71], A. Garcia-Bellido[71], V. Gavrilov[38], P. Gay[13], W. Geist[19], W. Geng[15,65], C.E. Gerber[51], Y. Gershtein[49,b], D. Gillberg[6], G. Ginther[50,71], B. Gómez[8], A. Goussiou[82], P.D. Grannis[72], S. Greder[19], H. Greenlee[50], Z.D. Greenwood[60], E.M. Gregores[4], G. Grenier[20], Ph. Gris[13], J.-F. Grivaz[16], A. Grohsjean[18], S. Grünendahl[50], M.W. Grünewald[31], F. Guo[72], J. Guo[72], G. Gutierrez[50], P. Gutierrez[75], A. Haas[70], P. Haefner[26], S. Hagopian[49], J. Haley[68], I. Hall[65], R.E. Hall[47], L. Han[7], K. Harder[45], A. Harel[71], J.M. Hauptman[57], J. Hays[44], T. Hebbeker[21], D. Hedin[52], J.G. Hegeman[35], A.P. Heinson[48], U. Heintz[62], C. Hensel[24], I. Heredia-De La Cruz[34], K. Herner[64], G. Hesketh[63], M.D. Hildreth[55], R. Hirosky[81], T. Hoang[49], J.D. Hobbs[72], B. Hoeneisen[12], M. Hohlfeld[22], S. Hossain[75], P. Houben[35], Y. Hu[72], Z. Hubacek[10], N. Huske[17], V. Hynek[10], I. Iashvili[69], R. Illingworth[50], A.S. Ito[50], S. Jabeen[62], M. Jaffré[16], S. Jain[75], K. Jakobs[23], D. Jamin[15], R. Jesik[44], K. Johns[46], C. Johnson[70], M. Johnson[50], D. Johnston[67], A. Jonckheere[50], P. Jonsson[44], A. Juste[50], E. Kajfasz[15], D. Karmanov[39], P.A. Kasper[50], I. Katsanos[67], V. Kaushik[78], R. Kehoe[79], S. Kermiche[15], N. Khalatyan[50], A. Khanov[76], A. Kharchilava[69], Y.N. Kharzheev[37], D. Khatidze[70], T.J. Kim[32], M.H. Kirby[53], M. Kirsch[21], B. Klima[50], J.M. Kohli[28], J.-P. Konrath[23], A.V. Kozelov[40], J. Kraus[65], T. Kuhl[25], A. Kumar[69], A. Kupco[11], T. Kurča[20], V.A. Kuzmin[39], J. Kvita[9], F. Lacroix[13], D. Lam[55], S. Lammers[54], G. Landsberg[77], P. Lebrun[20], W.M. Lee[50], A. Leflat[39], J. Lellouch[17], J. Li[78,‡], L. Li[48], Q.Z. Li[50], S.M. Lietti[5], J.K. Lim[32], D. Lincoln[50], J. Linnemann[65], V.V. Lipaev[40], R. Lipton[50], Y. Liu[7], Z. Liu[6], A. Lobodenko[41], M. Lokajicek[11], P. Love[43], H.J. Lubatti[82], R. Luna-Garcia[34,d], A.L. Lyon[50], A.K.A. Maciel[2], D. Mackin[80], P. Mättig[27], R. Magaña-Villalba[34], A. Magerkurth[64], P.K. Mal[46], H.B. Malbouisson[3], S. Malik[67], V.L. Malyshev[37], Y. Maravin[59], B. Martin[14], R. McCarthy[72], C.L. McGivern[58], M.M. Meijer[36], A. Melnitchouk[66], L. Mendoza[8], D. Menezes[52], P.G. Mercadante[5], M. Merkin[39], K.W. Merritt[50], A. Meyer[21], J. Meyer[24], J. Mitrevski[70], N.K. Mondal[30], R.W. Moore[6], T. Moulik[58], G.S. Muanza[15], M. Mulhearn[70], O. Mundal[22], L. Mundim[3], E. Nagy[15], M. Naimuddin[50], M. Narain[77], H.A. Neal[64], J.P. Negret[8], P. Neustroev[41], I. Nikolaev[71], H. Nilsen[23], H. Nogima[3], S.F. Novaes[5], T. Nunnemann[26], G. Obrant[41], C. Ochando[16], D. Onoprienko[59], J. Orduna[34], N. Oshima[50], N. Osman[44], J. Osta[55], R. Otec[10], G.J. Otero y Garzón[1], M. Owen[45], M. Padilla[48], P. Padley[80], M. Pangilinan[77], N. Parashar[56], S.-J. Park[24], S.K. Park[32], J. Parsons[70], R. Partridge[77], N. Parua[54], A. Patwa[73], G. Pawloski[80], B. Penning[23], M. Perfilov[39], K. Peters[45], Y. Peters[45], P. Pétroff[16], R. Piegaia[1], J. Piper[65], M.-A. Pleier[22], P.L.M. Podesta-Lerma[34,e], V.M. Podstavkov[50], Y. Pogorelov[55], M.-E. Pol[2], P. Polozov[38], A.V. Popov[40], W.L. Prado da Silva[3], S. Protopopescu[73], J. Qian[64], A. Quadt[24], B. Quinn[66], A. Rakitine[43],

M.S. Rangel[16], K. Ranjan[29], P.N. Ratoff[43], P. Renkel[79], P. Rich[45], M. Rijssenbeek[72], I. Ripp-Baudot[19], F. Rizatdinova[76], S. Robinson[44], M. Rominsky[75], C. Royon[18], P. Rubinov[50], R. Ruchti[55], G. Safronov[38], G. Sajot[14], A. Sánchez-Hernández[34], M.P. Sanders[26], B. Sanghi[50], G. Savage[50], L. Sawyer[60], T. Scanlon[44], D. Schaile[26], R.D. Schamberger[72], Y. Scheglov[41], H. Schellman[53], T. Schliephake[27], S. Schlobohm[82], C. Schwanenberger[45], R. Schwienhorst[65], J. Sekaric[49], H. Severini[75], E. Shabalina[24], M. Shamim[59], V. Shary[18], A.A. Shchukin[40], R.K. Shivpuri[29], V. Siccardi[19], V. Simak[10], V. Sirotenko[50], P. Skubic[75], P. Slattery[71], D. Smirnov[55], G.R. Snow[67], J. Snow[74], S. Snyder[73], S. Söldner-Rembold[45], L. Sonnenschein[21], A. Sopczak[43], M. Sosebee[78], K. Soustruznik[9], B. Spurlock[78], J. Stark[14], V. Stolin[38], D.A. Stoyanova[40], J. Strandberg[64], M.A. Strang[69], E. Strauss[72], M. Strauss[75], R. Ströhmer[26], D. Strom[53], L. Stutte[50], S. Sumowidagdo[49], P. Svoisky[36], M. Takahashi[45], A. Tanasijczuk[1], W. Taylor[6], B. Tiller[26], M. Titov[18], V.V. Tokmenin[37], I. Torchiani[23], D. Tsybychev[72], B. Tuchming[18], C. Tully[68], P.M. Tuts[70], R. Unalan[65], L. Uvarov[41], S. Uvarov[41], S. Uzunyan[52], P.J. van den Berg[35], R. Van Kooten[54], W.M. van Leeuwen[35], N. Varelas[51], E.W. Varnes[46], I.A. Vasilyev[40], P. Verdier[20], L.S. Vertogradov[37], M. Verzocchi[50], D. Vilanova[18], P. Vint[44], P. Vokac[10], M. Voutilainen[67,f], R. Wagner[68], H.D. Wahl[49], M.H.L.S. Wang[71], J. Warchol[55], G. Watts[82], M. Wayne[55], G. Weber[25], M. Weber[50,g], L. Welty-Rieger[54], A. Wenger[23,h], M. Wetstein[61], A. White[78], D. Wicke[25], M.R.J. Williams[43], G.W. Wilson[58], S.J. Wimpenny[48], M. Wobisch[60], D.R. Wood[63], T.R. Wyatt[45], Y. Xie[77], C. Xu[64], S. Yacoob[53], R. Yamada[50], W.-C. Yang[45], T. Yasuda[50], Y.A. Yatsunenko[37], Z. Ye[50], H. Yin[7], K. Yip[73], H.D. Yoo[77], S.W. Youn[53], J. Yu[78], C. Zeitnitz[27], S. Zelitch[81], T. Zhao[82], B. Zhou[64], J. Zhu[72], M. Zielinski[71], D. Zieminska[54], L. Zivkovic[70], V. Zutshi[52], and E.G. Zverev[39]

(The DØ Collaboration)

[1]*Universidad de Buenos Aires, Buenos Aires, Argentina*
[2]*LAFEX, Centro Brasileiro de Pesquisas Físicas, Rio de Janeiro, Brazil*
[3]*Universidade do Estado do Rio de Janeiro, Rio de Janeiro, Brazil*
[4]*Universidade Federal do ABC, Santo André, Brazil*
[5]*Instituto de Física Teórica, Universidade Estadual Paulista, São Paulo, Brazil*
[6]*University of Alberta, Edmonton, Alberta, Canada; Simon Fraser University,*
Burnaby, British Columbia, Canada; York University, Toronto,
Ontario, Canada and McGill University, Montreal, Quebec, Canada
[7]*University of Science and Technology of China, Hefei, People's Republic of China*
[8]*Universidad de los Andes, Bogotá, Colombia*
[9]*Center for Particle Physics, Charles University,*
Faculty of Mathematics and Physics, Prague, Czech Republic
[10]*Czech Technical University in Prague, Prague, Czech Republic*
[11]*Center for Particle Physics, Institute of Physics,*
Academy of Sciences of the Czech Republic, Prague, Czech Republic
[12]*Universidad San Francisco de Quito, Quito, Ecuador*
[13]*LPC, Université Blaise Pascal, CNRS/IN2P3, Clermont, France*
[14]*LPSC, Université Joseph Fourier Grenoble 1, CNRS/IN2P3,*
Institut National Polytechnique de Grenoble, Grenoble, France
[15]*CPPM, Aix-Marseille Université, CNRS/IN2P3, Marseille, France*
[16]*LAL, Université Paris-Sud, IN2P3/CNRS, Orsay, France*
[17]*LPNHE, IN2P3/CNRS, Universités Paris VI and VII, Paris, France*
[18]*CEA, Irfu, SPP, Saclay, France*
[19]*IPHC, Université de Strasbourg, CNRS/IN2P3, Strasbourg, France*
[20]*IPNL, Université Lyon 1, CNRS/IN2P3, Villeurbanne, France and Université de Lyon, Lyon, France*
[21]*III. Physikalisches Institut A, RWTH Aachen University, Aachen, Germany*
[22]*Physikalisches Institut, Universität Bonn, Bonn, Germany*
[23]*Physikalisches Institut, Universität Freiburg, Freiburg, Germany*
[24]*II. Physikalisches Institut, Georg-August-Universität Göttingen, Göttingen, Germany*
[25]*Institut für Physik, Universität Mainz, Mainz, Germany*
[26]*Ludwig-Maximilians-Universität München, München, Germany*
[27]*Fachbereich Physik, University of Wuppertal, Wuppertal, Germany*
[28]*Panjab University, Chandigarh, India*
[29]*Delhi University, Delhi, India*
[30]*Tata Institute of Fundamental Research, Mumbai, India*
[31]*University College Dublin, Dublin, Ireland*
[32]*Korea Detector Laboratory, Korea University, Seoul, Korea*
[33]*SungKyunKwan University, Suwon, Korea*
[34]*CINVESTAV, Mexico City, Mexico*

[35]*FOM-Institute NIKHEF and University of Amsterdam/NIKHEF, Amsterdam, The Netherlands*
[36]*Radboud University Nijmegen/NIKHEF, Nijmegen, The Netherlands*
[37]*Joint Institute for Nuclear Research, Dubna, Russia*
[38]*Institute for Theoretical and Experimental Physics, Moscow, Russia*
[39]*Moscow State University, Moscow, Russia*
[40]*Institute for High Energy Physics, Protvino, Russia*
[41]*Petersburg Nuclear Physics Institute, St. Petersburg, Russia*
[42]*Stockholm University, Stockholm, Sweden, and Uppsala University, Uppsala, Sweden*
[43]*Lancaster University, Lancaster, United Kingdom*
[44]*Imperial College, London, United Kingdom*
[45]*University of Manchester, Manchester, United Kingdom*
[46]*University of Arizona, Tucson, Arizona 85721, USA*
[47]*California State University, Fresno, California 93740, USA*
[48]*University of California, Riverside, California 92521, USA*
[49]*Florida State University, Tallahassee, Florida 32306, USA*
[50]*Fermi National Accelerator Laboratory, Batavia, Illinois 60510, USA*
[51]*University of Illinois at Chicago, Chicago, Illinois 60607, USA*
[52]*Northern Illinois University, DeKalb, Illinois 60115, USA*
[53]*Northwestern University, Evanston, Illinois 60208, USA*
[54]*Indiana University, Bloomington, Indiana 47405, USA*
[55]*University of Notre Dame, Notre Dame, Indiana 46556, USA*
[56]*Purdue University Calumet, Hammond, Indiana 46323, USA*
[57]*Iowa State University, Ames, Iowa 50011, USA*
[58]*University of Kansas, Lawrence, Kansas 66045, USA*
[59]*Kansas State University, Manhattan, Kansas 66506, USA*
[60]*Louisiana Tech University, Ruston, Louisiana 71272, USA*
[61]*University of Maryland, College Park, Maryland 20742, USA*
[62]*Boston University, Boston, Massachusetts 02215, USA*
[63]*Northeastern University, Boston, Massachusetts 02115, USA*
[64]*University of Michigan, Ann Arbor, Michigan 48109, USA*
[65]*Michigan State University, East Lansing, Michigan 48824, USA*
[66]*University of Mississippi, University, Mississippi 38677, USA*
[67]*University of Nebraska, Lincoln, Nebraska 68588, USA*
[68]*Princeton University, Princeton, New Jersey 08544, USA*
[69]*State University of New York, Buffalo, New York 14260, USA*
[70]*Columbia University, New York, New York 10027, USA*
[71]*University of Rochester, Rochester, New York 14627, USA*
[72]*State University of New York, Stony Brook, New York 11794, USA*
[73]*Brookhaven National Laboratory, Upton, New York 11973, USA*
[74]*Langston University, Langston, Oklahoma 73050, USA*
[75]*University of Oklahoma, Norman, Oklahoma 73019, USA*
[76]*Oklahoma State University, Stillwater, Oklahoma 74078, USA*
[77]*Brown University, Providence, Rhode Island 02912, USA*
[78]*University of Texas, Arlington, Texas 76019, USA*
[79]*Southern Methodist University, Dallas, Texas 75275, USA*
[80]*Rice University, Houston, Texas 77005, USA*
[81]*University of Virginia, Charlottesville, Virginia 22901, USA and*
[82]*University of Washington, Seattle, Washington 98195, USA*
(Dated: September 26, 2009)

We present a measurement of the mass difference between t and $\bar{t}$ quarks in lepton+jets final states of $t\bar{t}$ events in 1 fb^{-1} of data collected with the D0 detector from Fermilab Tevatron Collider $p\bar{p}$ collisions at $\sqrt{s} = 1.96$ TeV. The measured mass difference of 3.8 ± 3.7 GeV is consistent with the equality of t and $\bar{t}$ masses. This is the first direct measurement of a mass difference between a quark and its antiquark partner.

The CPT theorem [1], which is fundamental to any local Lorentz-invariant quantum field theory, requires that the mass of a particle and that of its antiparticle be identical. Tests of CPT invariance for many of the elementary particles accommodated within the standard model (SM) are available in the literature [2]. Despite the fact that no violations have ever been observed, it is important to search for the possibility of CPT violation in all sectors of the standard model. Because quarks carry color, they cannot be observed directly, but must first

evolve through quantum chromodynamic (QCD) interactions into jets of colorless particles. These jet remnants reflect the characteristics of the initially produced quarks, such as their charges, spin states, and masses. If the lifetimes of quarks are much longer than the time scale for QCD processes, the quarks form hadrons before they emerge from collisions, and decay from within bound hadronic states. This makes it difficult to measure a $q - \overline{q}$ mass difference because of the model dependence of QCD binding and evolution processes. However, since the lifetime of the top quark is far shorter than the time scale for QCD interactions, the top-quark sector provides a way to measure the mass difference less ambiguously [3].

In this Letter, we report a measurement of the difference between the mass of the top quark (t) and that of its antiparticle ($\overline{t}$) produced in $p\overline{p}$ collisions at $\sqrt{s} =$ 1.96 TeV. Our measurement is based on data corresponding to $\sim$1 fb^{-1} of integrated luminosity collected with the D0 detector [4] during Run II of the Fermilab Tevatron Collider. The events used in this analysis, identical to those in Ref. [5], are top quark pair ($t\overline{t}$) events in the lepton + jets channel (ℓ+jets) where each top quark is assumed to always decay into a W boson and a b quark. One of the W bosons decays via $W \rightarrow \ell\nu$ into two leptons, and the other one through $W \rightarrow q\overline{q}'$ into two quarks, and all four quarks ($q\overline{q}'b\overline{b}$) evolve into jets.

We select events having one isolated electron (muon) with transverse momentum $p_T > 20$ GeV and $|\eta| < 1.1$ ($|\eta| < 2$), missing transverse momentum $\not{p}_T > 20$ GeV, and exactly four jets with $p_T > 20$ GeV and $|\eta| < 2.5$, where the pseudorapidity $\eta = -\ln[\tan(\theta/2)]$, and θ is the polar angle with respect to the proton beam direction. At least one of the jets is required to be identified as a b-jet candidate. A minimum azimuthal separation is required between lepton p_T and $\not{p}_T$ vectors to further reduce multijet background arising from lepton or jet energy mismeasurements. The positively (negatively) charged leptons are used to tag the t ($\overline{t}$) in each event. To reduce instrumental effects that can cause charge dependent asymmetries in lepton energy scale and resolution, solenoid and toroid magnetic field polarities are routinely reversed.

The selected data sample consists of 110 e+jets and 110 μ+jets events. The W^+ (W^-) boson decays into hadrons in 105 (115) events and into leptons in 115 (105) events, consistent with invariance under charge conjugation. The fraction of $t\overline{t}$ events in this sample is estimated to be 74%. The background consists of W+jets and multijet events, with the latter comprising 12% of the entire background.

This analysis uses the matrix element (ME) method which relies on the extraction of the properties of the top quark (e.g., the mass) through a likelihood technique based on probability densities (PD) for each event, calculated from the ME for the two major processes ($t\overline{t}$ and W+jets production) that contribute to the selected

ℓ+jets sample. In calculating the PD for $t\overline{t}$ production, we include only the leading order (LO) ME from $q\overline{q} \rightarrow t\overline{t}$ production [6]. We assume SM-like $t\overline{t}$ production and decay, where identical particle and antiparticle masses are assumed for b quarks and W bosons but not for top quarks. For W+jets production, we use the ME provided in VECBOS [7]. The PD for each event is given in terms of the fraction of signal (f) and of background ($1 - f$) in the data and the masses of the t (m_t) and the $\overline{t}$ ($m_{\overline{t}}$):

$$P_{\text{evt}} = A(x)[fP_{\text{sig}}(x; m_t, m_{\overline{t}}) + (1 - f)P_{\text{bkg}}(x)] , \quad (1)$$

where x denotes the measured jet and lepton energies and angles, $A(x)$ is a function only of x and accounts for the geometrical acceptance and efficiencies, and P_{sig} and P_{bkg} represent the PD for $t\overline{t}$ and W+jets production, respectively. Multijet events are also represented by P_{bkg} since $P_{\text{bkg}} \gg P_{\text{sig}}$ for such events [8].

The free parameters in Eq. 1 are determined from a likelihood $L(x; m_t, m_{\overline{t}}, f)$ constructed from the product of the P_{evt} for all events. Jet energies are scaled by an overall jet energy scale (JES) calibration factor derived by constraining the reconstructed mass of the two jets from $W \rightarrow q\overline{q}'$ decays in $t\overline{t}$ events to 80.4 GeV [2, 5]. The likelihood is maximized as a function of f for each (m_t,$m_{\overline{t}}$) hypothesis to determine f^{best}. An integration of the likelihood for $f = f^{\text{best}}$ over the sum $m_{\text{sum}} = (m_t + m_{\overline{t}})/2$ results in a one-dimensional likelihood $L(x; \Delta)$ as a function of mass difference $\Delta = m_t - m_{\overline{t}}$. This is used to extract the mean value of Δ and its uncertainty. A similar procedure involving an integration over Δ gives $L(x; m_{\text{sum}})$ which is used to extract the mean value of m_{sum} and its uncertainty.

The variables in any ME refer to nascent produced particles (leptons and partons), but the measured quantities correspond to physical leptons and jets. This difference is taken into account in the calculation of the event probability by convoluting over phase space a transfer function, $W(y, x)$, that provides the resolution for the lepton in question or a mapping of the observed jet variables in an event (x) to their progenitor parton variables (y):

$$P_{\text{sig}} = \frac{1}{\sigma_{\text{norm}}^{t\overline{t}}}$$
$$\times \int \sum d\sigma(y; m_t, m_{\overline{t}})dq_1 dq_2 F(q_1)F(q_2)W(y, x),$$
$$(2)$$

where $d\sigma(y; m_t, m_{\overline{t}})$ is the leading-order partonic differential cross section, q_1 and q_2 are the momentum fractions of the colliding partons (assumed to be massless) within the incident p and $\overline{p}$, and the sum runs over all possible combinations of initial-state parton flavors, jet-to-parton assignments, and all $W \rightarrow \ell\nu$ neutrino solutions [9]. In the sum over jet-to-parton assignments in P_{sig}, each permutation of jets carries a weight w_i, which is the normalized product of probabilities for tagging any
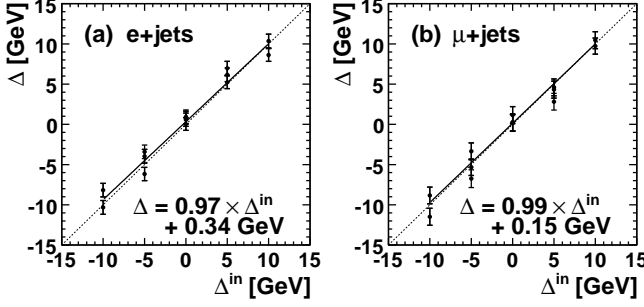
FIG. 1: Values of the measured mean Δ from MC pseudo experiments as a function of Δ^{in}, parameterized by straight lines for (a) e+jets and (b) μ+jets MC events. Dotted lines represent complete equality between measured and input values. Results from pseudo experiments with same Δ^{in} but different m_{sum} correspond to the extra points for fixed Δ^{in} (see text).
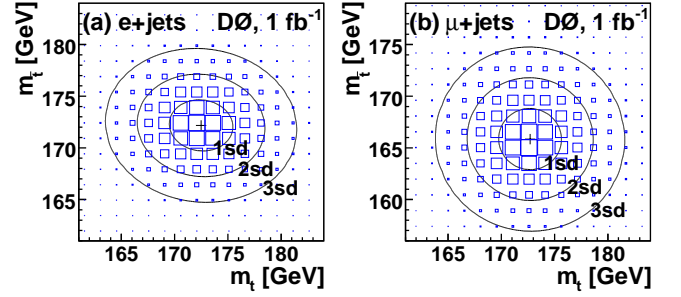

FIG. 2: Fitted contours of equal probability for the two-dimensional likelihoods as a function of m_t and $m_{\bar{t}}$ for (a) e+jets and (b) μ+jets data. The boxes, representing the bins in the two-dimensional histograms of the likelihoods, have areas proportional to the bin contents, set equal to the value of the likelihood evaluated at the bin center.

jet under a given parton flavor hypothesis [5]. The $F(q_i)$ include the probability densities for finding a parton of given flavor and longitudinal momentum fraction in the p or $\overline{p}$ assuming the CTEQ6L1 [10] parton distribution functions (PDF), as well as the probability densities for the transverse components of the q_i obtained from the LO event generator PYTHIA [11]. The normalization term $\sigma_{\mathrm{norm}}^{t\bar{t}}$ is described below.

The overall detection efficiency for $t\bar{t}$ depends on the values of both m_t and $m_{\bar{t}}$. This is taken into account through the normalization by the observed cross section $\sigma_{\mathrm{norm}}^{t\bar{t}} = \int A(x)P_{\mathrm{sig}}dx = \sigma^{t\bar{t}}(m_t, m_{\bar{t}}) \langle A(m_t, m_{\bar{t}}) \rangle$, where $\sigma^{t\bar{t}}(m_t, m_{\bar{t}})$ is the total cross section calculated by integrating the partonic cross section $\sigma_{q\bar{q}}^{t\bar{t}}$ [12], corresponding to the specific ME used in the analysis, over initial and final parton distributions and summing over initial parton flavors. $\langle A(m_t, m_{\bar{t}}) \rangle$ is the mean acceptance determined from the generated $t\bar{t}$ events. The expressions for P_{bkg} are similar, except that the probability does not depend on m_t or $m_{\bar{t}}$.

Samples of $t\bar{t}$ MC events with different values of m_t and $m_{\bar{t}}$ are required to simulate $t\bar{t}$ production and decay in order to calibrate the results of the analysis. These events are generated with a version of the PYTHIA generator [11] modified to provide independent values of m_t and $m_{\bar{t}}$. The specific values chosen for $(m_t, m_{\bar{t}})$ form a square grid spaced at 5 GeV intervals between (165,165) and (180,180), excluding the two extreme points at (165,180) and (180,165). The MC events for equal values of m_t and $m_{\bar{t}}$ are generated with the default version of PYTHIA.

Approximations made in formulating the likelihood can bias the final result. This issue is examined by comparing the measured and input values of Δ in pseudo experiments composed of MC $t\bar{t}$ and W+jets events. The calibration is shown in Fig. 1 in terms of the measured mean Δ as a function of its input value (Δ^{in}), separately for the e+jets and μ+jets MC samples, for all MC samples generated at the input reference points on the $(m_t,$

$m_{\bar{t}})$ grid. There are 2, 3, 4, 3, and 2 different $(m_t, m_{\bar{t}})$ points with a common Δ^{in} of -10, -5, 0, $+5$, and $+10$ GeV, respectively. The dispersions in the measured values of mean Δ for different $(m_t, m_{\bar{t}})$ points, but with same values of Δ^{in}, are consistent with expected statistical fluctuations, as can be observed in Fig. 1. The fit χ^2/d.o.f. for the points in Figs. 1(a) and 1(b) are 1.8 and 0.84, respectively. The parameterizations shown in Fig. 1 are used to calibrate $L(x; \Delta)$ for the selected data sample.

We define the pull as $(\Delta - \langle\Delta\rangle)/\sigma(\Delta)$ where Δ is the measured mass difference for a given pseudo experiment, $\langle\Delta\rangle$ is the mean measured mass difference for all pseudo experiments, and $\sigma(\Delta)$ is the uncertainty of the measured mass difference for the given pseudo experiment. The mean widths of the pull distributions for all samples used in Fig. 1 are 1.2 and 1.1 for e+jets and μ+jets, respectively. The deviations of these widths from 1 are used to correct the measured uncertainties in data.

Fitted two-dimensional Gaussian contours of equal probability (in terms of the standard deviation sd) for $L(x; m_t, m_{\bar{t}})$ are shown for the electron and muon data samples in Figs. 2(a) and 2(b), respectively. The corresponding $L(x; \Delta)$ for both channels are given in Figs. 3(a) and 3(b). The two sets of data are consistent within their respective uncertainties, and the small correlations ($\rho^{e+\mathrm{jets}} = -0.05$, $\rho^{\mu+\mathrm{jets}} = -0.01$) extracted from the fits in Fig. 2 between m_t and $m_{\bar{t}}$ are not statistically significant, nor are the shifts in the projections shown in Fig. 3.

Results from the two channels are combined through a weighted average of the separate electron and muon values. This has the advantage of using their respective pulls to adjust the uncertainties of each measurement before combining the two results. Using this averaging process, we quote the final combined means and their statistical uncertainties as $\Delta = 3.8 \pm 3.4(\mathrm{stat.})$ GeV and $m_{\mathrm{sum}} = 170.9 \pm 1.5(\mathrm{stat.})$ GeV. The latter is consistent
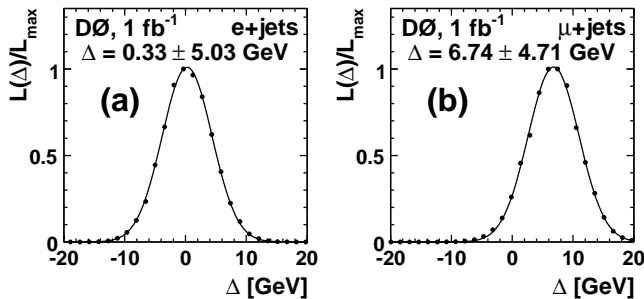
FIG. 3: Projections of the likelihoods onto the Δ axis for (a) e+jets and (b) μ+jets data.

TABLE I: Summary of systematic uncertainties on Δ.

Source	Uncertainty (GeV)
Physics modeling	
Signal	± 0.85
PDF uncertainty	± 0.26
Background modeling	± 0.03
Heavy flavor scale factor	± 0.07
b fragmentation	± 0.12
Detector modeling:	
b/light response ratio	± 0.04
Jet identification	± 0.16
Jet resolution	± 0.39
Trigger	± 0.09
Overall jet energy scale	± 0.08
Residual jet energy scale	± 0.07
Muon resolution	± 0.09
Wrong charge leptons	± 0.07
Asymmetry in $b\bar{b}$ response	± 0.42
Method:	
MC calibration	± 0.25
b-tagging efficiency	± 0.25
Multijet contamination	± 0.40
Signal fraction	± 0.10
Total (in quadrature)	± 1.22

with the previous measurement of Ref. [5] (see also Ref. [13]).

The systematic uncertainties are summarized in Table I. The first category, *Physics modeling*, comprises the uncertainties in MC modeling of $t\bar{t}$ and W+jets events. The second category, *Detector modeling*, addresses uncertainties in the calibration of jet energy and simulation of detector response. The last category, *Method*, addresses uncertainties in the calibration and possible systematic effects due to assumptions made in the analysis. Except for two, all systematic uncertainties are identical to those described previously [5]. Many of these uncertainties (e.g., uncertainties in JES, PDF, jet resolution, multijet contamination) are expected to partially cancel in the measurement of the mass difference, but are often dominated by the statistics of the samples used to evaluate them. The two new contributions address the possibilities of (i) reconstructing leptons with the wrong charge, and (ii) uncertainties from modeling differences in the response of the calorimeter to b and $\bar{b}$ jets [14], which can affect the measurement of the mass difference. These were evaluated for (i) by estimating the effect of an increase in charge misidentification in MC simulations that would match that found in data ($\sim 1\%$ for both e and μ). For (ii), studies were performed on MC samples and on data seeking any difference in detector response to b and $\bar{b}$ quarks beyond expectations from interactions of their decay products, which are accommodated in the MC simulations. The observed differences were limited by the statistics of both samples. The total systematic uncertainty is 1.2 GeV. Combining the systematic and statistical uncertainties of the measurement in quadrature yields $\Delta = 3.8 \pm 3.7$ GeV, a value consistent with CPT invariance.

In summary, we have measured the t and $\bar{t}$ mass difference in ~ 1 fb^{-1} of data in ℓ+jets $t\bar{t}$ events and find the mass difference to be $m_t - m_{\bar{t}} = 3.8 \pm 3.7$ GeV, corresponding to a relative mass difference of $\Delta/m_{\mathrm{sum}} = (2.2 \pm 2.2)\%$. This is the first direct measurement of a mass difference between a quark and its antiquark partner.

[a] Visitor from Augustana College, Sioux Falls, SD, USA.
[b] Visitor from Rutgers University, Piscataway, NJ, USA.
[c] Visitor from The University of Liverpool, Liverpool, UK.
[d] Visitor from Centro de Investigacion en Computacion - IPN, Mexico City, Mexico.
[e] Visitor from ECFM, Universidad Autonoma de Sinaloa, Culiacán, Mexico.
[f] Visitor from Helsinki Institute of Physics, Helsinki, Finland.
[g] Visitor from Universität Bern, Bern, Switzerland.
[h] Visitor from Universität Zürich, Zürich, Switzerland.
[‡] Deceased.

[1] J. Schwinger, Phys. Rev. **82**, 914 (1951); G. Luders, K. Dan. Vidensk. Selsk. Mat. Fys. Medd. **28**, 5 (1954); *Niels*

Bohr and the Development of Physics, edited by W. Pauli (McGraw-Hill, New York, 1955), p. 30; D. Colladay and V.A. Kostelecky, Phys. Rev. D **55**, 6760 (1997); J.S. Bell, Proc. R. Soc. **A231**, 479 (1955).

[2] C. Amsler *et al.* (Particle Data Group), Phys. Lett. B **667**, 93 (2008).

[3] J.A.R. Cembranos, A. Rajaraman, and F. Takayama, Europhys. Lett. **82**, 21001 (2008).

[4] V.M. Abazov *et al.* (D0 Collaboration), Nucl. Instrum. Methods Phys. Res., Sect. A **565**, 463 (2006).

[5] V.M. Abazov *et al.* (D0 Collaboration), Phys. Rev. Lett. **101**, 182001 (2008).

[6] V. Abazov *et al.* (D0 Collaboration), Phys. Rev. D **74**, 092005 (2006).

[7] F.A. Berends *et al.*, Nucl. Phys. **B357**, 32 (1991).

[8] When this is satisfied, the relative contribution of P_{sig} to P_{evt} will be negligible for such events, minimizing their influence in the determination of m_t and $m_{\overline{t}}$.

[9] The transverse components of the unmeasured ν momentum p_ν are determined from the p_T balance of the $t\overline{t}$ event, but the remaining ambiguity in the longitudinal component of p_ν leaves more than one possibility or "solution" for p_ν.

[10] J. Pumplin *et al.* (CTEQ Collaboration), JHEP **0207**, 012 (2002).

[11] T. Sjöstrand *et al.*, Comput. Phys. Commun. **135**, 238 (2001).

[12] $\sigma_{q\overline{q}}^{t\overline{t}} = \frac{8\pi\alpha_s^2}{27s^{5/2}}p(3E_t^2 + 3E_{\overline{t}}^2 + 2p^2 + 6m_t m_{\overline{t}})$ where α_s is the strong coupling constant, s is the square of the center-of-mass energy in the incoming $q\overline{q}$ rest frame, and E_i and p are the energies of the t or $\overline{t}$ and their common momentum, respectively, in the $q\overline{q}$ frame.

[13] The result in Ref. [5] was obtained by further constraining the jet energy scale to the one derived from photon+jets and dijet samples. This constraint is not used in the present analysis since it shifts m_t and $m_{\overline{t}}$ in the same way and has no effect on Δ.

[14] Differences in the composition of b and $\overline{b}$ jets, such as different K^+/K^- fractions, can cause differences in calorimeter response because of differences in K^+/K^- interaction cross sections.